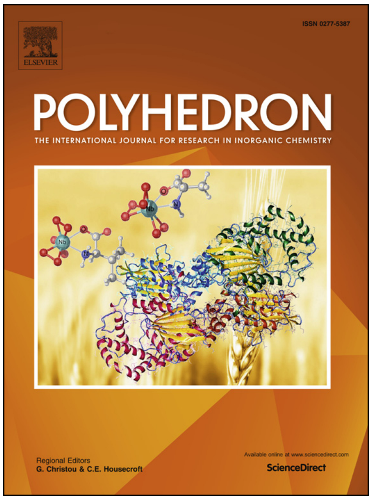

Synthesis and Structures of Bis(iminophosphorano)methanide Chelate Complexes with Zinc and Group 13

Jin Zhang, Sai Ge, Jianguo Zhao, Imran Ulhaq, Micheal J. Ferguson, Robert McDonald, Guibin Ma, Cavell G. Ronald

PII: S0277-5387(18)30781-2
DOI: https://doi.org/10.1016/j.poly.2018.11.056
Reference: POLY 13603

To appear in: *Polyhedron*

Received Date: 26 September 2018
Accepted Date: 26 November 2018

Please cite this article as: J. Zhang, S. Ge, J. Zhao, I. Ulhaq, M.J. Ferguson, R. McDonald, G. Ma, C.G. Ronald, Synthesis and Structures of Bis(iminophosphorano)methanide Chelate Complexes with Zinc and Group 13, *Polyhedron* (2018), doi: https://doi.org/10.1016/j.poly.2018.11.056

Synthesis and Structures of Bis(iminophosphorano)methanide Chelate Complexes with Zinc and Group 13

Jin Zhang[1], Sai Ge[1], Jianguo Zhao[1*], Imran Ulhaq[2], Micheal J. Ferguson[2], Robert McDonald[2], Guibin Ma[1,2*] and Cavell G Ronald[2]

[1]Institute of Carbon Materials Science, Shanxi Datong University, Datong, Shanxi Province, 037009, PR China

[2]Chemistry Department, University of Alberta, Edmonton, Alberta, T6G 2G2, Canada

[*]Corresponding Author's E-mail address: jgzhaoshi@163.com (Prof. J. Zhao) or guibin@ualberta.ca (Dr. G. Ma)

Abstract: The organolithium bis(iminophosphorano)methandiide dimer $[Li_2C(Ph_2P{=}NSiMe_3)_2]_2$ ($[Li_2$-**1**$]_2$) reacts with 4 equiv of $AlCl_3$ in THF to generate the novel bimetallic aluminum carbene complex of $[Li(THF)_4][\{C(Ph_2P{=}NSiMe_3)_2\}Al_2Cl_5]$ (**1**). In addition, several new bis(iminophosphorano)methanide chelate-coordinated complexes of $[\{CH(Ph_2P{=}NSiMe_3)_2\}AlCl_2]$ **(2)**, $[\{CH(Ph_2P{=}NSiMe_3)_2\}GaBr_2]$ **(3)**, $[\{CH(Ph_2P{=}NSiMe_3)_2\}InCl_2]$ **(4)**, and $[\{CH(Ph_2P{=}NSiMe_3)_2\}InBr_2]$ **(5)** are synthesized in situ while organolithium bis(iminophosphorano)methandiide ($[Li_2$-**1**$]_2$) reacts with 2 equiv of metal halides $AlCl_3$, $GaBr_3$ $InCl_3$ and $InBr_3$ respectively in THF. Furthermore, an unexpected complex of $[\{CH_2(Ph_2P{=}NSiMe_3)_2\}ZnCl_2]$ **(6)** is formed as $[Li_2$-**1**$]_2$ dimer reacted with 2 equiv of $ZnCl_2$ in situ. All six synthesized complexes (**1**, **2**, **3**, **4**, **5** and **6**) in situ were isolated in solid and were structurally characterized by X-ray diffraction. Complexes containing particular carbene to metal or ionic linking interaction bonds (**1**, **2**, **3** and **4**) were selected and further characterized in detail by DFT calculations using Gaussian03 program. The DFT calculation demonstrates the existence of a carbene-Al σ bond in structure **1** and ionic linkage interaction in structures **2-4**.

Keywords: bis(iminophosphorano)methandiide dimer, organolithium, aluminum, gallium, indium, zinc, DFT calculation.

Introduction

Metal complexes with chelate ligands have continued to attract scientific attention and generated a considerable amount of interest in chemicals as well as catalytic applications [1]. We [2] and others [3] have developed a chelate N,N-bidentate monoanionic of bis(diphenyliminophosphorano)methanide (LiHL) or bianionic bis(diphenyliminophosphorano) methandiide (Li_2L) ligand systems several years ago through either single or double deprotonation of bis(diphenyliminophosphorano)methane with lithium methide (**Scheme 1**).

Scheme 1

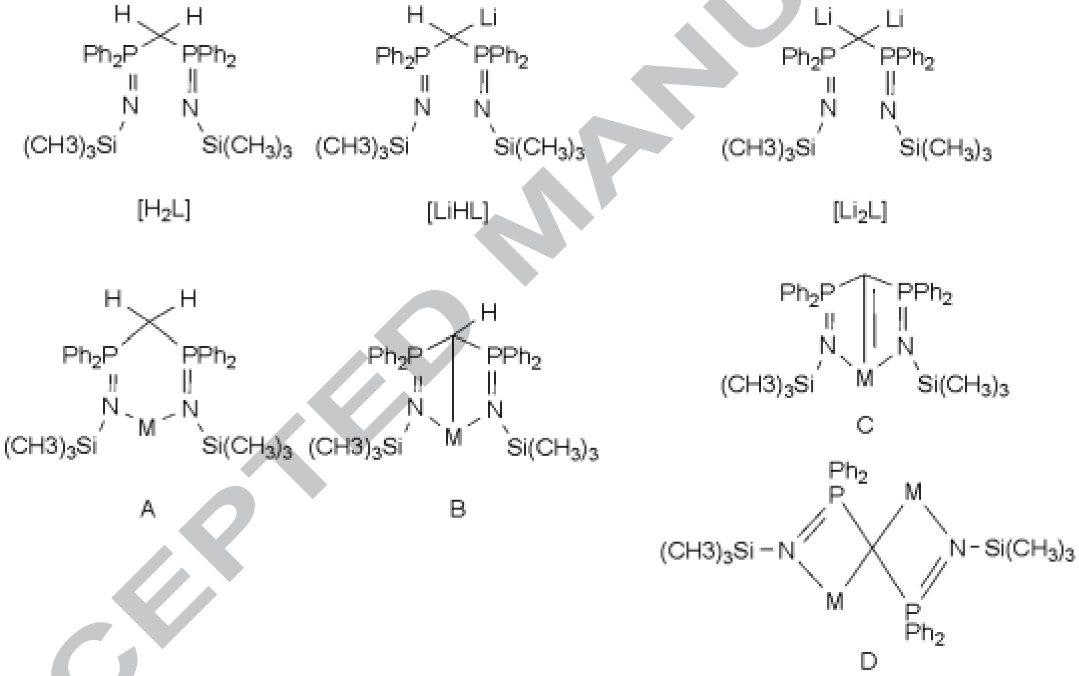

It was demonstrated that our ligand systems have abundant chemical bonding properties and reactivities with transition metals, lanthanide and actinide metals, as well as main group elements. E.g. formation complexes containing either single (C−M) or double (C=M) carbene−metal bonds, or formation of monomeric and bimetallic complexes, which showed great catalytic activities (**Scheme** 1)[4]. We have learned from our synthesis experiments that the reactivities of these ligand systems, especially dilithium Li_2L salt, are pretty much dependent on the structures of metal precursors. In addition, the metal properties and electronic configurations are critical factors for how well the carbene will bind to the metal, through formation of either a single or double bond between the carbene carbon and metal center. Compared to transition and lanthanide metals, the chemistry of these chelate ligands with main group elements have not been extensively explored. A few examples of Al^{3+} and Tl^{+} metals were conducted in our laboratory so far [5], showing unusual reactivities and catalytic activities, especially for Al complexes [6]. To further understand the reactivities of this type of ligands with structural examples, especially with rarely studied closed shell main group elements, we have extended our ligand system to main group 13 elements and a few bis(diphenyliminophosphorano)methandiide, bis(diphenyliminophosphorano)methanide and bis(diphenyliminophosphorano)methane chelate coordinated Al^{3+}, Ga^{3+}, In^{3+} and Zn^{2+} complexes. Complexes containing a six-member-ring in boat conformation were prepared, isolated and structurally characterized by X-ray diffraction and DFT calculations.

Experimental Section

General Considerations. All manipulations were performed either in an Ar-filled glove box or under an Ar or N_2 atmosphere using standard Schlenk techniques. Solvents were dried over appropriate drying agents and degassed by three freeze-pump-thaw cycles prior to use. The organolithium compounds [Li_2-**1**]$_2$ was prepared according to our published procedures [2]. NMR spectra were recorded at ambient temperature using THF-d_8 or toluene-d_8 solutions of the complexes on a Varian i400 spectrometer (161.9 MHz for ^{31}P, 100.6 MHz for ^{13}C) and referenced to residual solvent proton (^{1}H), solvent (^{13}C), external 85% H_3PO_4 (^{31}P). Elemental analyses were carried out at Analytical and Instrumentation Laboratory, Department of Chemistry, University of Alberta.

Synthesis of [{$C(Ph_2P{=}NSiMe_3)_2$}Al_2Cl_5][$Li(C_4H_8O)_4$] (1)

To THF solution (10 ml) of [Li_2-1]$_2$ (0.115 g, 0.10 mmol) was added $AlCl_3$ (0.054 g, 0.40 mmol) as a solid in a single portion at room temperature. The resulting solution was stirred at room temperature overnight, during which the mixture turned into a clear light yellow solution. The filtered THF solution was evaporated on a dynamic vacuum line and the remaining powder was dissolved in 5 ml ether. The undissolved solid of LiCl was removed by centrifugation. The yellow-green solution was evaporated under vacuum to half of the volume and a few drops of dry toluene was added. The solution was kept inside the freezer (-20° C) for a few days, during which white crystals formed. The top liquid was taken and dried under vacuum. The product of **1** was obtained (0.124 g, yield 57.2%). Anal. Calcd for $C_{47}H_{70}Al_2Cl_5LiN_2O_4P_2Si_2$: C, 52.11; H, 6.51; N, 2.59. Found: C, 52.0; H, 6.67; N, 2.61. ^{1}H NMR: ^{1}H NMR(THF-d_8): δ 7.94 (t, phenyl, 8H), 7.69 (d, phenyl, 4H), 7.35 (t, phenyl, 8H), −0.24 (s, -Si(C**H**$_3$)$_3$, 18H). ^{13}C{^{1}H, ^{31}P} NMR (THF-d_8): δ 135.71(s, phenyl), 133.68(s, phenyl), 132.22(s, phenyl), 128.18(s, phenyl), 3.31 (s, Si(**C**H$_3$)$_3$). ^{31}P{^{1}H} NMR(THF-d_8): δ 35.98 (s).

Synthesis of [{CH(Ph$_2$P=NSiMe$_3$)$_2$}AlCl$_2$] (2)

To THF solution (10 ml) of [Li$_2$-1]$_2$ (0.115 g, 0.10 mmol) was added $AlCl_3$ (0.027 g, 0.20 mmol) as a solid in a single portion at room temperature. The isolation procedure was similar as **1.** The product of **2** was obtained (0.085 g, yield 65%). Anal. Calcd for $C_{31}H_{39}AlCl_2N_2P_2Si_2$: C, 56.79; H, 6.00; N, 4.27. Found: C, 56.65; H, 6.03; N, 4.25. ^{1}H NMR(THF-d_8): δ 7.82 (t, phenyl, 8H), 7.34 (d, phenyl, 4H), 7.10 (t, phenyl, 8H), −0.12 (s, -Si(C**H**$_3$)$_3$, 18H). ^{13}C{^{1}H, ^{31}P} NMR (THF-d_8): δ 132.7(s, phenyl), 131.3(s, phenyl), 129.7(s, phenyl), 127.0(s, phenyl), 3.82 (s, Si(**C**H$_3$)$_3$). ^{31}P{^{1}H} NMR(THF-d_8): δ 29.88 (s).

Synthesis of [{CH(Ph$_2$P=NSiMe$_3$)$_2$}GaBr$_2$] (3)

To THF solution (10 ml) of [Li$_2$-1]$_2$ (0.115 g, 0.10 mmol) was added $GaBr_3$ (0.062 g, 0.20 mmol) as a solid in a single portion at room temperature. The isolation procedure was similar as **1**. The product of **3** was obtained (0.118 g, yield 75%). Anal. Calcd for $C_{31}H_{39}Br_2GaN_2P_2Si_2$: C, 47.29; H, 4.99; N, 3.56. Found: C, 47.50; H, 5.01; N, 3.53. ^{1}H NMR(THF-d_8): δ 7.70 (t, phenyl, 8H), 7.34 (d, phenyl, 4H), 7.30 (t, phenyl, 8H), −0.13 (s, -Si(C**H**$_3$)$_3$, 18H). ^{13}C{^{1}H, ^{31}P} NMR (THF-d_8): δ 137.05(s, phenyl), 134.51(s, phenyl), 129.65(s, phenyl), 3.56 (s, Si(**C**H$_3$)$_3$). ^{31}P{^{1}H} NMR(THF-d_8): δ 31.68 (s).

Synthesis of [{CH(Ph$_2$P=NSiMe$_3$)$_2$}InCl$_2$] (4)

To THF solution (10 ml) of [Li_2-1]$_2$ (0.115 g, 0.10 mmol) was added $InCl_3$ (0.044 g, 0.20 mmol) as a solid in a single portion at room temperature. The isolation procedure was similar as **1**. The product of **4** was obtained (0.116 g, yield 79%). Anal. Calcd for $C_{31}H_{39}Cl_2N_2P_2Si_2In$: C, 50.08; H, 5.29; N, 3.77. Found: C, 50.31; H, 5.27; N, 3.88. ^{1}H NMR: ^{1}H NMR(THF-d_8): δ 7.62 (t, phenyl, 8H), 7.36 (d, phenyl, 4H), 7.25 (t, phenyl, 8H), −0.03 (s, -Si(C**H**$_3$)$_3$, 18H). ^{13}C{^{1}H, ^{31}P} NMR (THF-d_8): δ 132.29(s, phenyl), 131.35(s, phenyl), 128.32 (s, phenyl), 3.47 (s, Si(**C**H$_3$)$_3$). ^{31}P{^{1}H} NMR(THF-d_8): δ 33.2 (s).

Synthesis of [{CH(Ph_2P=NSiMe$_3$)$_2$}InBr$_2$] (5)

To THF solution (10 ml) of [Li_2-1]$_2$ (0.115 g, 0.10 mmol) was added $InBr_3$ (0.071 g, 0.20 mmol) as a solid in a single portion at room temperature. The isolation procedure was similar as **1**. The product of **5** was obtained (0.123 g, yield 74%). Anal. Calcd for $C_{31}H_{39}Br_2InN_2P_2Si_2$: C, 44.73; H, 4.72; N, 3.37. Found: C, 44.68; H, 4.64; N, 3.32. ^{1}H NMR ($CDCl_3$): δ 7.60 (t, phenyl, 8H), 7.36 (d, phenyl, 4H), 7.26 (t, phenyl, 8H), −0.02 (s, -Si(C**H**$_3$)$_3$, 18H). ^{13}C{^{1}H, ^{31}P} NMR ($CDCl_3$): δ 133.89(s, phenyl), 132.51(s, phenyl), 131.22(s, phenyl), 128.24(s, phenyl), 3.62 (s, Si(**C**H$_3$)$_3$). ^{31}P{^{1}H} NMR($CDCl_3$): δ 32.92 (s).

Synthesis of [{CH$_2$(Ph_2P=NSiMe$_3$)$_2$}ZnCl$_2$] (6)

To THF solution (10 ml) of [Li_2-1]$_2$ (0.115 g, 0.10 mmol) was added $ZnCl_2$ (0.028 g, 0.20 mmol) as a solid in a single portion at room temperature. The isolation procedure was similar as **1**. The product of **6** was obtained (0.112 g, yield 80%). Anal. Calcd for $C_{31}H_{40}Cl_2N_2P_2Si_2Zn$: C, 53.57; H, 5.80; N, 4.03. Found: C, 53.84; H, 5.78; N, 4.05. ^{1}H NMR: ^{1}H NMR(THF-d_8): δ 7.48 (q, phenyl, 8H), 7.32 (t, phenyl, 4H), 7.22 (t, phenyl, 8H), −0.094 (s, -Si(C**H**$_3$)$_3$, 18H). ^{13}C{^{1}H, ^{31}P} NMR (THF-d_8): δ 137.51(s, phenyl), 131.36(s, phenyl), 129.71(s, phenyl), 127.45(s, phenyl), 3.25 (s, Si(**C**H$_3$)$_3$). ^{31}P{^{1}H} NMR(THF-d_8): δ 30.78 (s).

Crystal Structure Determination. Suitable crystals of **1** to **6** were mounted on glass fibers by means of mineral oil, and data were collected using graphite-monochromated

MoKα radiation (0.71073 Å) on a Bruker PLATFORM/ SMART 1000 CCD diffractometer. The structure was solved by direct methods using *SHELXL-90* [11a], and refined using full-matrix least-squares on F^2 (*SHELXL-93*) [11b]. All non-hydrogen atoms in the structure compound were refined with anisotropic displacement parameters. Selected crystal data and structure refinement details for **1-6** are listed in **Table** 1.

Computational Details. The geometric optimization and energy calculations were performed with the Gaussian03 program [10a] based on the density functional theory (DFT) method. The Becke's three-parameter hybrid functional with the Lee-Yang-Parr correlation functional (B3LYP) [12] was employed for all calculations. For geometric optimization, the LANL2DZ basis sets for Ga, In and 6-31G(d) for others. Once an optimized geometry was obtained, imaginary frequencies were checked at the same level by vibration analysis to verify the genuine minimum on the potential energy surface (PES) and to evaluate the zero-point energy (ZPE) correction. The DFT wave functions obtained at optimized structures were confirmed to be stable. Gaussian NBO analysis was carried out for the final optimized structures [10b].

Results and Discussion

Synthesis and Crystal Structures

Transmetalation of the lithium methandiide complex, $[Li_2C(Ph_2P{=}NSiMe_3)_2]_2$ ($[Li_2L]_2$), with $AlCl_3$ in a 1:4 molar ratio in THF followed by extraction with ether and crystallization from ether/toluene afforded the corresponding aluminum complex $[Li(THF)_4][\{C(Ph_2P{=}NSiMe_3)_2\}Al_2Cl_5]$ (**1**) as colorless crystals in good yield (**Scheme** 2). Complex of $[\{CH(Ph_2P{=}NSiMe_3)_2\}AlCl_2]$ (**2**) was isolated as crystalline solid from the reactant solution of $[Li_2L]_2$ with $AlCl_3$ salts in 1:2 molar ratio in THF. This compound was prepared by reaction of $[LiHC(Ph_2P{=}NSiMe_3)_2]$ with $AlCl_3$ in benzene [4s]. In a similar procedure, the bis(iminophosphorano)methanide complexes of $[\{CH(Ph_2P{=}NSiMe_3)_2\}GaBr_2]$ (**3**), $[\{CH(Ph_2P{=}NSiMe_3)_2\}InCl_2]$ (**4**), $[\{CH(Ph_2P{=}NSiMe_3)_2\}InBr_2]$ (**5**) and $[\{CH_2(Ph_2P{=}NSiMe_3)_2\}ZnCl_2]$ **(6)** were synthesized by reaction of $[Li_2L]_2$ with the corresponding metal halides in situ and isolated in solid (**Scheme** 3).

Scheme 2

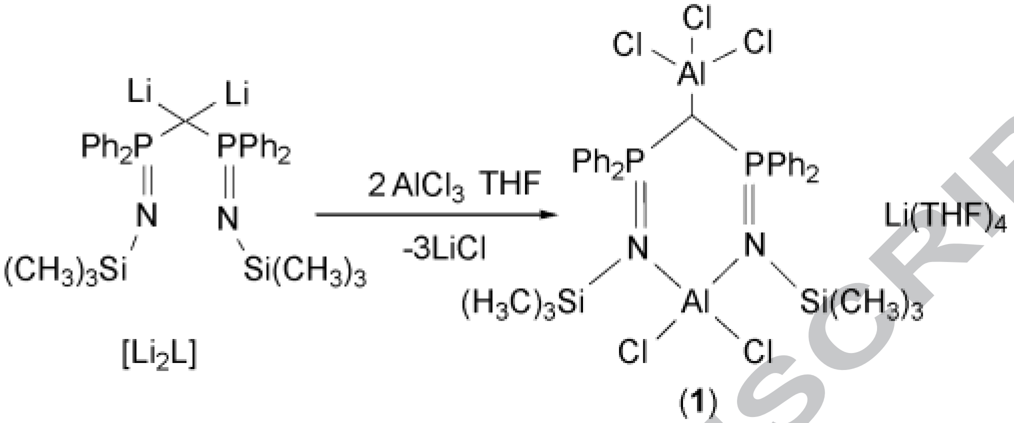

Scheme 3

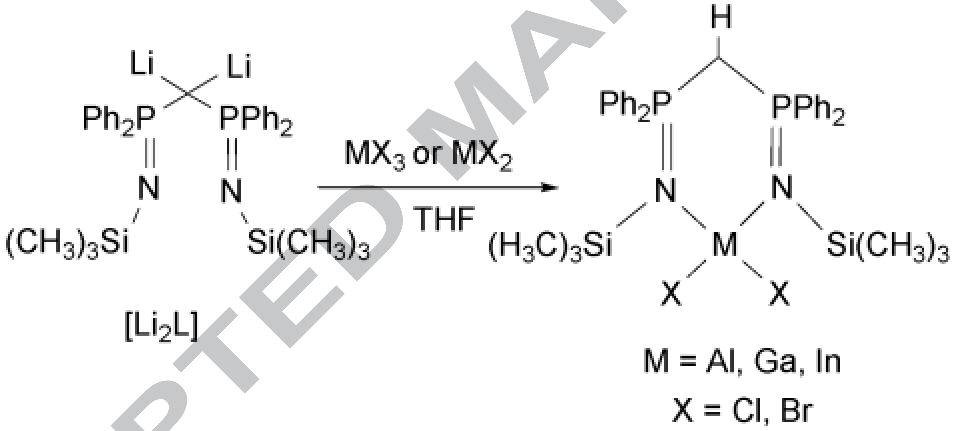

The solid structure of **1** was investigated by single-crystal X-ray diffraction (**Figure** 1). Compound **1** is a bimetallic organometallic carbene compound and crystallizes in the triclinic space group *P*ī, with two molecules in the unit cell. The selected bond lengths and angles are given in Table 2. Two nitrogen atoms coordinate to Al(1) and generates the heteroatomic six-member ring (-Al(1)-N(1)-P(1)-C(1)-N(2)-P(2)-). Four atoms of P(1)-N(1)-N(2)-P(2) sit in a perfect plane, while Al(1) and C(1) are located above this plane to form a boat conformation. At the front of the boat, two chelate nitrogen atoms (N(1) and N(2)), and two chlorine atoms (Cl(1) and Cl(2)) coordinate to Al(1). At the tail of the boat, PCP carbene center coordinates to Al(2) with three chlorine atoms (Cl(3), Cl(4) and Cl(5)). Both aluminum centers (Al(1) and Al(2)) adapt to a slightly twisted tetrahedral geometry as expected. In addition, four atoms of carbene and its bonded three atoms (P(1), P(2) and Al(2)) are almost within one plane as well. The bond length of carbene-Al (Al(2)-C(1) = 1.966(4) Å) is shorter than the NHC heterocyclic carbene aluminum structure (Al-C = 2.009(5)) [7], which has the same coordination environment as **1** (C $AlCl_3$). The bond lengths of Al-C (Al(2)-C(1) = 1.966(4) Å), Al-N (Al(1)-N(1) =1.866(3), and Al(1)-N(2) = 1.871(3) Å) in **1** are notably shorter in comparison with our previously determined carbon bridged two aluminum compound [5b] $[(Me_2Al)_2C(Ph_2P{=}NSiMe_3)_2]_2$ (average Al-N = 1.930(3) Å) and Al-C = 2.119(3) Å), which indicates a strong bonding interaction in **1**.

Scheme 4

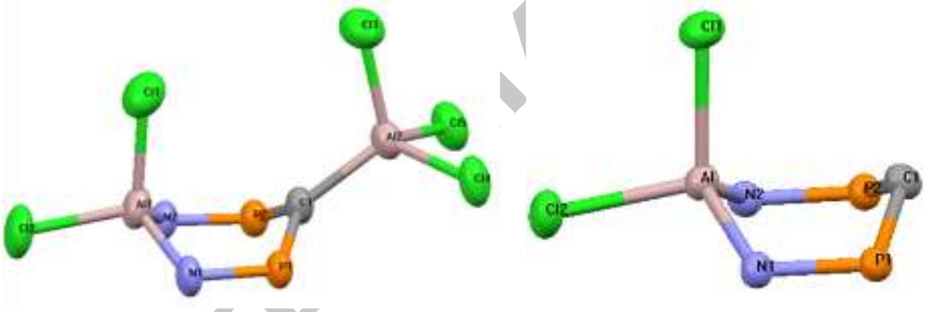

One aluminum bis(diphenyliminophosphorano)methanide compound of $[\{CH(Ph_2P{=}NSiMe_3)_2\}AlCl_2]$ **(2)** was isolated and the crystal structure solved by X-ray diffraction (**Figure** 2). The core structural conformation of **2** is compatible to **1** with similar bond lengths (**Scheme** 4 and **Table** 2). Instead of carbene coordinated to $AlCl_3$ as shown in **1** with one protonated H in **2**. The C(1)---Al distance of 2.763(3) Å is considerably longer than the Al-C bonding lengths, indicating there is no direct bonding interaction. However, it is notably shorter than the C(1)-Al(1) distance in **1** (C(1)-Al(1) = 2.957(3) Å), suggesting some ionic link interaction between positive charge (Al) and negative charge (C(1)), which is supposed non-existent in the structure **1** between C(1) and Al(1).

The crystal structures of **3** to **5** were all solved using X-ray diffraction (see **Figure** 3 to **Figure** 5; selected bond lengths and angles in **Table** 2). To the best of our knowledge, the crystal structures even with the preparation of indium metal compounds with this type ligand have not been reported in literature. However, one structure of [{CH(Ph$_2$P=NSiMe$_3$)$_2$}GaCl$_2$] was previously determined [4s] for the gallium metal. The solid structure of **3** [{ ^{2}-CH(Ph$_2$P=NSiMe$_3$)$_2$}GaBr$_2$] is in the same space group as that of the previously reported chloride coordinated compound, with compatible Ga-N bond lengths and N-Ga-N angle as well as the same boat conformation [4s]. The pseudotetrahedral coordination sphere about Ga is defined by the two phosphinimine nitrogen atoms and the two bromides. The “bite angle” of the bisphosphinimine anion is 113.88(14)°, while the Br(1)-Ga-Br(2) angle is 105.29(2)°. The distance between C(1) with charge (-1) and Ga with charge (+1) (2.913(3) Å) is shorter than Al(1)-C(1) distance in structure **1** (2.957(3) Å) regardless of the long Ga-N bonds in structure **3**, which indicates the existence of ionic link interaction within **3** as similarly presented in **2**. Structures of two indium compounds with chloride (**4**) and bromide (**5**) are similar to each other, both having the same conformation as **2** and **3**. Based on the atomic distances between C(1) and In within the molecular structures (2.763(3) Å (**4**) and 2.803(3) Å (**5**)), it clearly indicates the existence of ionic linkage interaction.

The crystal structure of zinc compound **6** is shown in **Figure** 6 and the selected bond lengths and angles are listed in **Table** 2. The zinc coordination sphere as expected is pseudotetrahedral with two nitrogen atoms and chlorides, but the structure is not identical to **2**-**5**, whereas the carbon is single protonated. The distance between C(1) and zinc within the heterocyclic six-member ring, C(1)-Zn = 3.156(3) Å, is the longest compared with structures **2**-**5**, which points to a lack of ionic link interaction in **6**. This is further understood as **6** is neutral, and ionic linkage interaction can only exist when there is positive/negative charge separation.

The structural features of the determined crystal structures are all analogous to formation of the heterocyclic six-member ring (CP$_2$N$_2$M, M = Al, Ga, In and Zn) as boat conformation. In contrast to the conformation of **1**, the boat shape of **2** is more flat with larger N(1)-Al-N(2) and P(1)-C(1)-P(2) angles and shorter distances of C(1) and Al above the P$_2$N$_2$ plane (Table 2). This could be due to the C(1)—Al distance shrinkage caused by attraction interaction between the negative charge around C(1) and positive charge around Al. It is interesting to note that in analogous structures **2**-**5**, the N(1)-M-N(2) and P(1)-C(1)-P(2) bond angles are almost identical in compounds **2** and **3** for Al and Ga, and in compounds **4** and **5** for In, no matter where chloride or bromide coordinates to the metals. However, these two angles (N(1)-M-N(2) and P(1)-C(1)-P(2), M = Zn) were the smallest (**Table** 2) in **6**, which also had the longest C(1)-M (M = Zn) atomic distance (3.156(3) Å) compared to structures (**2**-**5**, from 2.763(3) to 2.913(3) Å). These differences between **2**-**5** and **6** indicate the existence of an attraction interaction between separated positive and negative charges within molecules in **2**-**5**, which could cause shrinking of distance C(1)-M and eventually enlarge the two angles.

Both of the P-C(carbon) lengths in **1**-**5** are noticeably shorter than that found for parent P-C(carbon) in H_2-**1** [8] (P(1)-C(1) = 1.708(2) ~ 1.7289(3) vs 1.827(1) Å), while the P-N distances are considerably longer (P(1)-N(1) and P(2)-N(2) = 1.6260(15) ~ 1.647(3) vs 1.539(2) Å). The electronically delocalized effect inside the heterocyclic 6-membered ring introduces a structural bond length difference between H_2-**1** and bound **1**-**5**. This observation is similar to our previously studied complexes and consistent with our suggestion of -electron delocalization discussed previously [4i, 4h, 4k, 4n, 4o, 9].

DFT Calculations

The interested bonding model molecules, $[\{C(Me_2P{=}NSiH_3)_2\}Al_2Cl_5]^-$ (**1a**), $[\{HC(Me_2P{=}NSiH_3)_2\}AlCl_2]$ (**2a**) containing Al-carbene bond, $[\{HC(Me_2P{=}NSiH_3)_2\}GaBr_2]$ (**3a**) and $[\{HC(Me_2P{=}NSiH_3)_2\}InCl_2]$ (**4a**) presenting ionic linkage interactions, were selected and further characterized by Gaussian-03 DFT calculations as well as NBO analysis for **1a** [10]. The HOMO of four model structures is shown in **Figure** 7, it is seen that **1a** is obviously different than those of **2a**-**4a**. Based on the molecular orbital coefficients (MOCs), it can be explained that the bonding interaction to metals of carbene (P_2C) is different than its protonated (P_2CH) carbon. **1a** to **4a** all contain the σ bond between carbon and two P by overlapping their p_z atomic orbitals. In addition to the σ bond, **2a** to **4a** also have nonbonding free electron of p_y atomic orbital around the carbon, making the surface of the molecular orbital electron shell unsymmetric as shown in **Figure** 7. This finding is in agreement with the crystal structures that show there is one remaining negative charge around the carbon center.

Unlike structures **2a-4a** which are similar in bonding, **1a** is a novel aluminum carbene compound. The NBO analysis was performed on this novelty structure. After geometry optimization calculation, the structural data show that two of P-C, P-N and N-Al bond lengths are identical within the six-membered ring, while two Cl-Al bond lengths around Al(1) are not equivalent (see SI). Two of the three Cl-Al bond lengths around Al(2) are equivalent but not identical to the third one (See SI), which is in agreement with the crystal structural data (**1**). NBO analysis shows around Al(2) metal that the carbene-Al bond is 13.3% from the Al(2) $s^{0.33}p^{0.67}$ hybrid orbital and 86.7% from the carbene $s^{0.32}p^{0.68}$ hybrid orbital, while the two Cl(4), Cl(5) to Al(2) is 86.4% Cl $s^{0.37}p^{0.63}$ and 13.6% Al(2) $s^{0.23}p^{0.77}$ hybrid orbitals respectively and Cl(3)-Al(2) is 86.1% from Cl $s^{0.36}p^{0.64}$ and 13.9% from Al(2) $s^{0.24}p^{0.76}$ as well. For Al(1) metal center, N-Al is 8.3% from Al $s^{0.29}p^{0.71}$ and 91.7% from N $s^{0.33}p^{0.67}$ hybrid orbital, and Cl(1)-Al(1) is 13.7% Al $s^{0.24}$ $p^{0.76}$ and 86.3% Cl $s^{0.36}p^{0.64}$ as well as Cl(2)-Al(1) is 13.5% Al $s^{0.22}p^{0.78}$ and 86.5% Cl $s^{0.38}p^{0.62}$ hybrid orbitals as shown in **Figure** 8 (details listed in SI).

Conclusions

The reactions of bis(diphenyliminophosphorano) methandiide (Li_2L) ligand with group 13 metals are conducted, and one stable air-sensitive carbene aluminum compound (**1**) was isolated and characterized by crystallography. Several novel unexpected complexes resulted as the final products of Ga and In metals. No carbene-metal bond formed after reaction with this bianionic electron rich ligand in situ, and eventually one protonated carbon coordinated compounds (**2**, **3**, **4** and **5**) was isolated in solid. This indicates that carbene bound Ga and In are not stable enough to hinder its protonated trend. As we know, the second proton of P-C**H**$^-$-P is more strongly bonded than the first proton in P-CH**H**-P, and the bianionic ligand (P-C^2-P) tends to back to P-C**H**-P while it is not strongly bound by a metal center, which is the case for Ga and In metals. As for Zn, both in reactions of H_2L with $Zn(CH_3)_2$ previously [4u] or Li_2L with $ZnCl_2$ herein, no species with carbene metal bond formation was generated. This study clearly demonstrates that the d orbital-filled main group 13 elements have different metal-bonding behavior than those of the transition metals lanthanides and actinides, while reacting with the electron rich PCP carbene ligand. In comparing the distance between C(1) and metal ions within the heterocyclic six-member ring of **1** and **6** to **2-5,** we have determined the existence of an ionic linkage or separation positive/negative charge attraction interaction in **2-5**.

Acknowledgement. We are grateful to Shanxi '1331 Project' Foundation for the Construction of Collaborative Innovation Center of Graphene Industrial Application. We also want to thank the Natural Sciences and Engineering Research Council (NSERC) of Canada for financial support of this work in terms of a Discovery Grant. The authors would like to thank the University of Alberta for support to maintain the X-Ray Crystallography, and Analytical and Instrumentation laboratories at the Department of Chemistry which were essential for this work.

Supporting Information Available: Crystallographic data (as CIF files) **1**-**6**, the different views of the structures (**Figures** S1-1 to S1-6) and selected bond distances and bond angles (**Table** S1-1 to S1-6) and some Gaussian calculation and NBO analysis data.

References:

[1] See for example: (a) S. W. Kohl, L. Weiner, L. Schwartsburd, L. Konstantinovski, L. J. Shimon, Y. Ben-David, M. A. Iron, D. Milstein, Consecutive thermal H_2 and light-induced O_2 evolution from water promoted by a metal complex, Science 324 (2009) 74-77 (DOI: 10.1126/science.1168600). (b) S. P. Green, C. Jones, A. Stasch, Stable magnesium(I) compounds with Mg-Mg bonds, Science 318 (2007) 1754-1757 (DOI: 10.1126/science.1150856).

[2] (a) K. Aparna, R. P. Kamalesh Babu, R. McDonald, R. G. Cavell, $[Ph_2P(NSiMe_3)]_2CLi_2$: A dilithium dianionic methanide salt with an unusual Li_4C_2 cluster structure, Angew. Chem. Int. Ed. 38 (1999) 1483-1484 (DOI: 10.1002/(SICI)1521-3773(19990517)38:10<1483::AID-ANIE1483>3.0.CO;2-D). (b) M. Klobukowski, S. A. Decker, C. C. Lovallo, R. G. Cavell, Structure and bonding in

an octahedral Li_4C_2 cluster, the dilithium bis {dihydrido(silylimino)phosphorano} methanide dimer. A combined DFT–AIM analysis, Theochem – J. Mol. Struct. 536 (2001) 189-194 (https://doi.org/10.1016/S0166-1280(00)00626-6).

[3] C. M. Ong, D. W. Stephan, Lithiations of bis-diphenyl-*N*-trimethylsilylphosphiniminomethane: An X-ray structure of a 1,1-dilithiomethane derivative, J. Am. Chem. Soc. 121(1999) 2939-2940 (DOI: 10.1021/ja9839421).

[4] See for example: Single C-M bond, (a) G. Aharonian, K. Feghali, S. Gambarotta, G. P. A. Yap, Stability of trivalent vanadium alkyl and hydride supported by a chelating phosphinimido ligand, Organometallics 20 (2001) 2616-2622 (DOI: 10.1021/om0101588). (b) S. T. Liddle, D. P. Mills, B. M. Gardner, J. McMaster, C. Jones, W. D. Woodul, A heterobimetallic gallyl complex containing an unsupported Ga−Y bond, Inorg. Chem. 48 (2009) 3520-3522 (DOI: 10.1021/ic900278t). (c) M. J. Sarsfield, H. Steele, M. Helliwell, S. J. Teat, Uranyl bis-iminophosphorane complexes with in- and out-of-plane equatorial coordination, Dalton Trans. (2003) 3443-3449 (DOI: 10.1039/B304602H). (d) G.-B. Ma, M. Ferguson, R. McDonald, R. G. Cavell, Rare, hexatomic, boat-shaped, cross-linked bis(iminodiphenylphosphorano)methanediide pincer carbon bridged photoluminescent copper clusters capped with methyl or halide bridges, Organometallics 29 (2010) 4251-4264 (DOI: 10.1021/om1002478). Double C=M bond: (e) S. T. Liddle, J. McMaster, J. C. Green, P. L. Arnold, Synthesis and structural characterisation of an yttrium–alkyl–alkylidene, Chem. Commun. (2008) 1747-1749 (DOI: 10.1039/B719633D). (f) K. Aparna, M. Ferguson, R. G. Cavell, A monomeric samarium bis(Iminophosphorano) chelate complex with a Sm=C bond, J. Am. Chem. Soc. 122 (2000) 726-727 (DOI: 10.1021/ja9936114). (g) R. P. Kamalesh Babu, R. McDonald, R. G. Cavell, Nucleophilic reactivity of the multiply bonded carbon center in group 4 pincer bis(iminophosphorano)methanediide complexes, Organometallics 19 (2000) 3462-3465 (DOI: 10.1021/om000181d). (h) R. P. Kamalesh Babu, R. McDonald, R. G. Cavell, The first hafnium methandiide complexes: the assembly of an entire triad of group 4 metal ‘pincer’ bis(phosphinimine) complexes possessing the M=C carbene–ylide structure, Chem. Commun. (2000) 481-482 (DOI: 10.1039/A909771F). (i) K. Aparna, R. P. Kamalesh Babu, R. McDonald, R. G. Cavell,

The first biscarbene complex of a group 4 metal: [Zr{C(Me$_2$P=NSiMe$_3$)$_2$}$_2$], Angew. Chem. Int. Edit. 40 (2001) 4400-4402 (https://doi.org/10.1002/1521-3773(20011203)40:23<4400::AID-ANIE4400>3.0.CO;2-W). (j) R. G. Cavell, R. P. Kamalesh Babu, K. Aparna, R. McDonald, Novel metal−carbon multiply bonded twelve-electron complexes of Ti and Zr supported by a bis(phosphoranimine) chelate, J. Am. Chem. Soc. 121 (1999) 5805-5806 (DOI: 10.1021/ja984087o). (k) G.-B. Ma, M. J. Ferguson, R. McDonald, R. G. Cavell, Actinide metals with multiple bonds to carbon: synthesis, characterization, and reactivity of U(IV) and Th(IV) bis(iminophosphorano)methandiide pincer carbene complexes, Inorg. Chem. 50 (2010) 6500-6508 (DOI: 10.1021/ic102537q). For example: Bimetallic: (l) K. Aparna, R. McDonald, R. G. Cavell, Chromium bis(phosphoranimine) complexes; bridging chromium carbenes with no CO or Cp supporting ligands, Chem. Commun. (1999) 1993-1994 (DOI: 10.1039/A905241K). (m) M. Fang, N. D. Jones, R. Lukowski, J. Tjathas, M. J. Ferguson, R. G. Cavell, A bimetallic, coordinated-ketene complex formed from a bimetallic lithium–carbon spirocycle by lithium-mediated insertion of CO into a rhodium–carbon bond, Angew. Chem. Int. Ed. 45 (2006) 3097-3101 (https://doi.org/10.1002/anie.200503814). (n) M. Fang, N. D. Jones, K. Friesen, G.-Y. Lin, M. J. Ferguson, R. McDonald, R. Lukowski, R. G. Cavell, Bimetallic, spirocyclic, methylene-bridged carbene complexes of rhodium and palladium derived by stepwise metalations of lithiated bis(diphenylphosphoranotrimethylsilylimido)methandiide, Organometallics, 28 (2009) 1652–1665 (DOI:10.1021/om8005678). (o) G.-B. Ma, R. McDonald, R. G. Cavell, A spirocyclic, bimetallic, carbon-bridged bis(iminophosphorano)methanediide complex of palladium(II): synthesis, crystal structure, solution behavior, and DFT bonding analysis, Organometallics 29 (2010) 52-60 (DOI: 10.1021/om900571k). For example: chelate six-member ring: (p) T. K. Panda, P. W. Roesky, P. Larsen, S. Zhang, C. Wickleder, Reactions of potassium bis(phosphinimino)methanide with group 11 compounds, Inorg. Chem. 45 (2006) 7503-7508 (DOI: 10.1021/ic060932p). (q) M. Rastätter, A. Zulys, P. W. Roesky, Bis(phosphinimino)methanide rare earth amides: synthesis, structure, and catalysis of hydroamination/cyclization, hydrosilylation, and sequential hydroamination/hydrosilylation, Chem. Eur. J. 13 (2007) 3606-3616 (https://doi.org/10.1002/chem.200601510). (r) C. M. One, P. McKarns, D. W. Stephan, Neutral and cationic group 13 phosphinimine and phosphinimide complexes, Organometallics 18 (1999) 4197-4204 (DOI: 10.1021/om9904044). (s) M. T. Gamer, S. Dehnen, P. W. Roesky, Synthesis and structure of yttrium and lanthanide bis(phosphinimino)methanides, Organometallics 20 (2001) 4230-4236 (DOI: 10.1021/om0102955). (t) K. Aparna, R. McDonald, R. G. Cavell, Structure and reactivity of a methyl zinc bis(iminophosphorano)methanide chelate complex, Organometallics 18 (1999) 3775-3777 (DOI: 10.1021/om990415x). (u) R. P. Kamalesh Babu, K. Aparna, R. McDonald, R. G. Cavell, Monomeric alkali metal (Li, Na, K) complexes of bis(iminophosphorano)methanides, Organometallics 20 (2001) 1451-1455 (DOI: 10.1021/om000982g). (v) M. T. Gamer, P. W. Roesky, I. Palard, M. L. Hellaye, S. M. Guillaume, In situ formation of bis(phosphinimino)methanide rare earth alkoxide initiators for the ring-opening polymerization of ε-caprolactone, Organometallics 26 (2007) 651-657 (DOI: 10.1021/om0608307). For example: Reviews: (w) R. G. Cavell, R. P. Kamalesh Babu, K. Aparna, Early transition metal and lanthanide bis(iminophosphorano)methandiide complexes; 'pincer' and bridging bis(phosphorus) metal carbenes, J. Organomet. Chem. 617 (2001) 158-169 (refs. therein) (https://doi.org/10.1016/S0022-328X(00)00735-X). (x) D. Morales-Morales, C. M. Jensen, (Editors) The Chemistry of Pincer Compounds, R. G. Cavell, Chapter 14, Pincers, Chelate and Spirocyclic Metal Carbene Complexes from Bis(iminophosphorano)methane Ligands, 2007, p: 311-346. Elsevier B. V.

[5] (a) K. Aparna, R. McDonald, R. G. Cavell, Carbon−carbon double bond formation Reactions of the unique spirocyclic aluminum bis(iminophosphorano)methandiide complex: Insertion of heteroallenes into aluminum-carbon bonds, J. Am. Chem. Soc. 122 (2000) 9314-9315 (DOI: 10.1021/ja001445q). (b) K. Aparna, R. McDonald, M. Ferguson, R. G. Cavell, Novel dialkyl aluminum bis(iminophosphorano)methanide and methanediide complexes, Organometallics 18 (1999) 4241-4243 (DOI: 10.1021/om990486w). (c) G.-B. Ma, M. Ferguson, R. G. Cavell, A geminal dithallated

bis(iminodiphenylphosphorano)methine carbon bridged dimer bound by Tl–Tl interactions, Chem Commun. 46 (2010) 5370-5372 (DOI: 10.1039/c0cc01088j).

[6] R. G. Cavell, K. Aparna, R. P. Kamalesh Babu, Q. Wang, Aluminum bis(iminophosphorano)methanide and methandiide complexes—transition metal-free ethylene polymerization cationic catalyst precursors, J. Mol. Catal. A, 189 (2002) 137-143 (https://doi.org/10.1016/S1381-1169(02)00205-4).

[7] A. Stasch, S. Singh, H. W. Roesky, M. Noltemeyer, H. G. Schmidt, Adducts of aluminum and gallium trichloride with a *N*-heterocyclic carbene and an adduct of aluminum trichloride with a thione, Eur. J. Inorg. Chem. (2004) 4052-4055 (DOI: 10.1002/ejic.200400247).

[8] A. Müller, M. Möhlen, B. Neumüller, N. Faza, W. Massa, K. Dehnicke, Crystal structures of the silylated phosphaneimines $Me_3SiNP(c\text{-}C_6H_{11})_3$ and $(Me_3SiNPPh_2)_2CH_2$, Z. Anorg. Allg. Chem. 625 (1999) 1748-1751.

[9] (a). R. P. Kamalesh Babu, R. McDonald, S. A. Decker, M. Klobukowski, R. G. Cavell, New zirconium hydrocarbyl bis(phosphoranimino) “pincer” carbene complexes, Organometallics 18 (1999) 4226-4229 (DOI: 10.1021/om9901473). (b) N. D. Jones, G. Lin, R. A. Gossage, R. McDonald, R. G. Cavell, Synthesis, structure, and reactivity of an unusual platinum olefin carbene complex, $[(\eta^4\text{-}cod)Pt\{=C(Ph_2P=NSiMe_3)_2\text{-}\kappa C,\kappa N\}]$, Organometallics 22 (2003) 2832-2841 (DOI: 10.1021/om030003v) [Erratum: Organometallics 22 (2003) 5378].

[10] (a) M. J. Frisch, G. W. Trucks, H. B. Schlegel, G. E. Scuseria, M. A. Robb, J. R. Cheeseman, V. G. Zakrzewski, J. A. Montgomery Jr, R. E. Stratmann, J. C. Burant, S. Dapprich, J. M. Millam, A. D. Daniels, K. N. Kudin, M. C. Strain, O. Farkas, J. Tomasi, V. Barone, M. Cossi, R. Cammi, B. Menucci, C. Pomelli, C. Adamo, S. Clifford, J. Ochterski, G. A. Petersson, P. Y. Ayala, Q. Cui, K. Morokuma, N. Rega, P. Salvador, J. J. Dannenberg, D. K. Malick, A. D. Rabuck, K. Raghavachari, J. B. Foresman, J. Cioslowski, J. V. Ortiz, G. Baboul, B. B. Stefanov, G. Liu, A. Liashenko, P. Piskorz, I. Komaromi, R. Gomperts, R. L. Martin, D. J. Fox, T. Keith, M. A. Al-Laham, C. Y. Peng, A. Nanayakkara, M. Challacombe, P. M. W. Gill, B. G. Johnson, W. Chen, M. W. Wong, J. L. Andres, C. Gonzalez, M. Head-Gordon, E. S. Replogle,

J. A. Pople, Revision C02 Gaussian, Inc., Pittsburgh PA, 2004. (b) E. D. Glendening, A. E. Reed, J. E. Carpenter, F. Weinhold, NBO version 3.1.

[11] (a) G. M. Sheldrick, Phase annealing in *SHELX*-90: Direct methods for larger structures, Acta Crystallogr. A46 (1990) 467-473 (https://doi.org/10.1107/S0108767390000277). (b) G. M. Sheldrick, *SHELXL*-93. Program for crystal structure determination. University of Göttingen, Germany, 1993.

[12] (a) A. D. Becke, Density-functional thermochemistry. III. The role of exact exchange, J. Chem. Phys. 98 (1993) 5648-5652 (https://doi.org/10.1063/1.464913). (b) C. Lee, W. Yang, R. G. Parr, Development of the Colle-Salvetti correlation-energy formula into a functional of the electron density, Phys. Rev. B 37 (1998) 785-789 (DOI: https://doi.org/10.1103/PhysRevB.37.785). (c) S. H. Vosko, L. Wilk, M. Nusair, Accurate spin-dependent electron liquid correlation energies for local spin density calculations: a critical analysis, Can. J. Phys. 58 (1980) 1200-1211(https://doi.org/10.1139/p80-159).

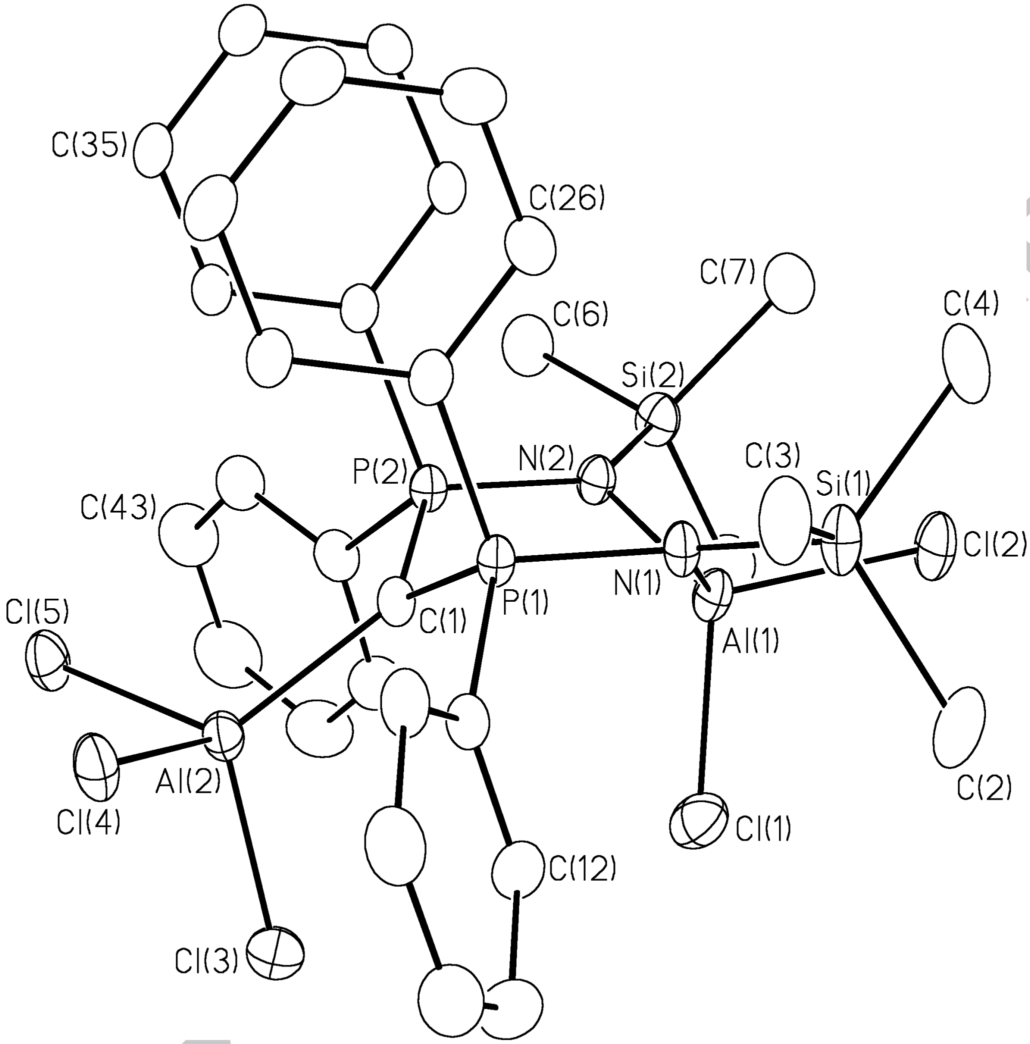

Figure 1. Perspective view of the $[\{C(Ph_2PNSiMe_3)_2\}Al_2Cl_5]^-$ anion showing the atom labeling scheme. Non-hydrogen atoms are represented by Gaussian ellipsoids at the 20% probability level. Hydrogen atoms are not shown.

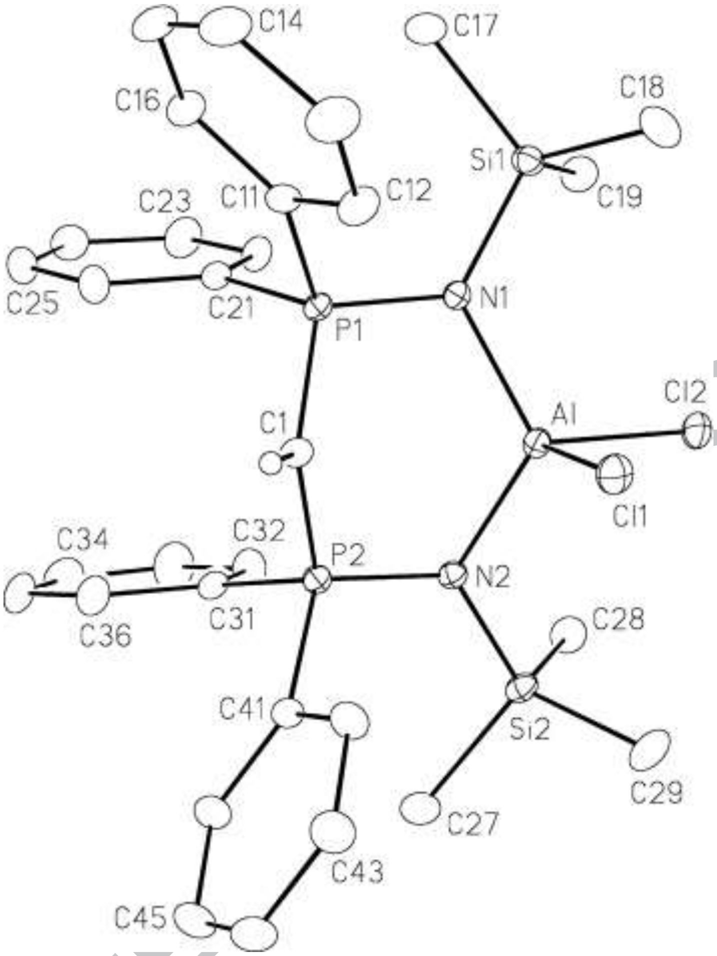

Figure 2. Perspective view of the $[Cl_2Al\{\kappa^2\text{–}HC(Ph_2PNSiMe_3)_2\}]$ molecule showing the atom labelling scheme. Non-hydrogen atoms are represented by Gaussian ellipsoids at the 20% probability level. The hydrogen atom attached to C(1) is shown with an arbitrarily small thermal parameter; all other hydrogens are not shown.

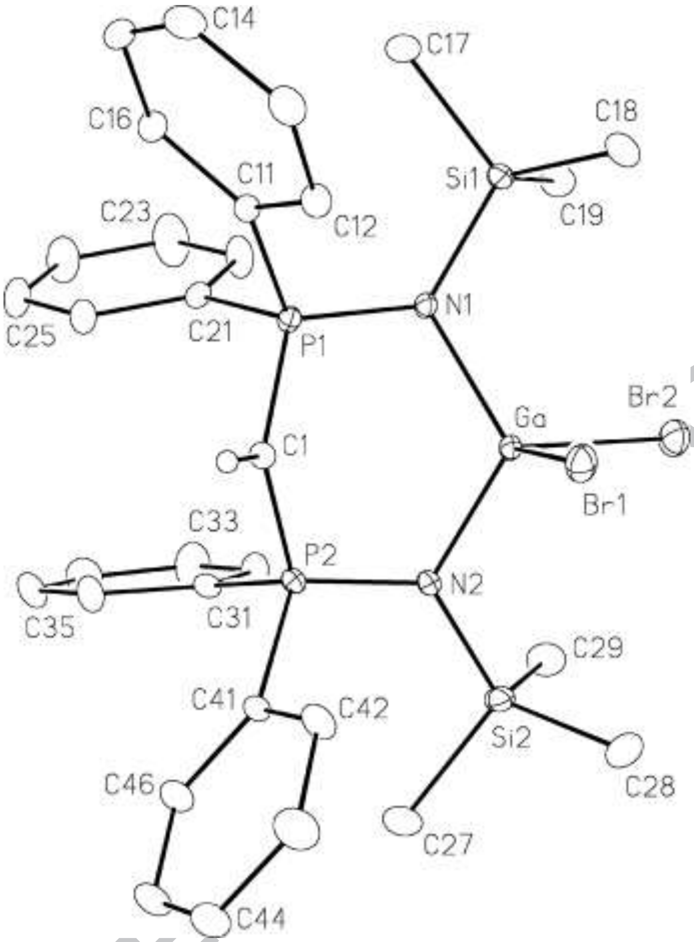

Figure 3. Perspective view of the [$Br_2Ga\{\kappa^2$–$HC(Ph_2PNSiMe_3)_2\}$] molecule showing the atom labelling scheme. Non-hydrogen atoms are represented by Gaussian ellipsoids at the 20% probability level. The hydrogen atom attached to C(1) is shown with an arbitrarily small thermal parameter; all other hydrogens are not shown.

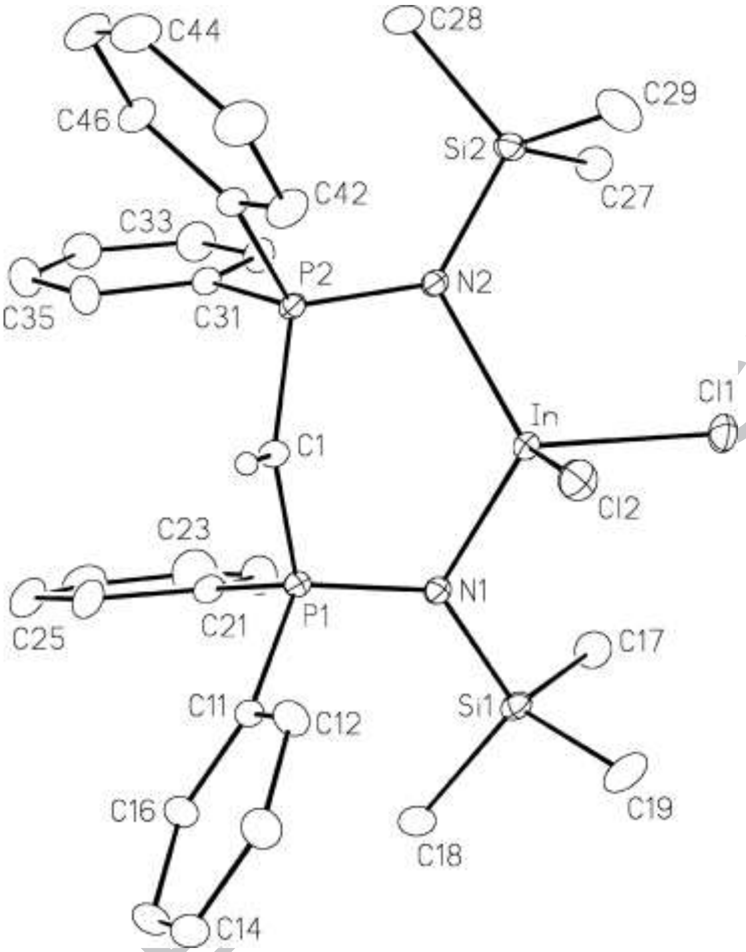

Figure 4. Perspective view of the [$Cl_2In\{\kappa^2–HC(Ph_2PNSiMe_3)_2\}$] molecule showing the atom labelling scheme. Non-hydrogen atoms are represented by Gaussian ellipsoids at the 20% probability level. The hydrogen atom attached to C(1) is shown with an arbitrarily small thermal parameter; all other hydrogens are not shown.

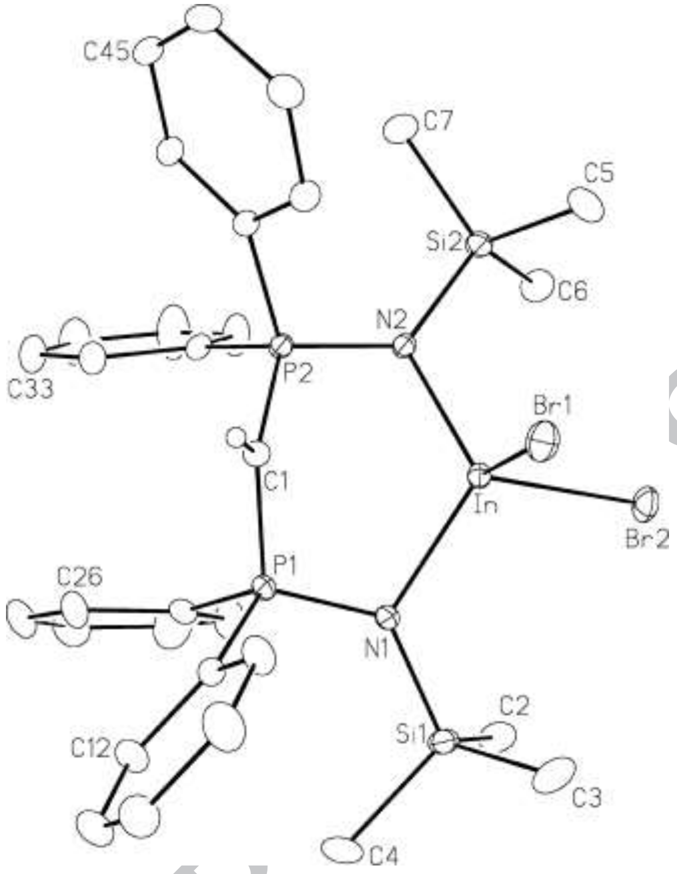

Figure 5. Perspective view of the $[\{CH(Ph_2PNSiMe_3)_2\}InBr_2]$ molecule showing the atom labelling scheme. Non-hydrogen atoms are represented by Gaussian ellipsoids at the 20% probability level. Only the methine hydrogen atom is shown (with arbitrarily small thermal parameter); all other hydrogen atoms are not shown.

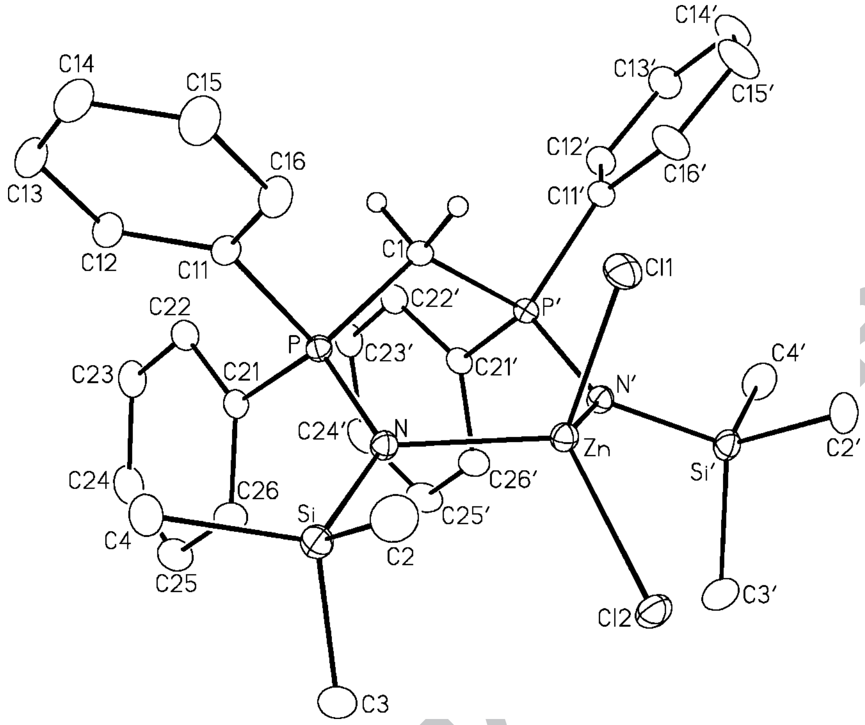

Figure 6. Perspective view of the $[\kappa^2\text{–}\{CH_2(Ph_2P{=}NSiMe_3)_2\}ZnCl_2]$ molecule showing the atom labelling scheme. Primed atoms are related to unprimed ones by the crystallographic mirror plane located at (*x*, ¼, *z*). Non-hydrogen atoms are represented by Gaussian ellipsoids at the 20% probability level.

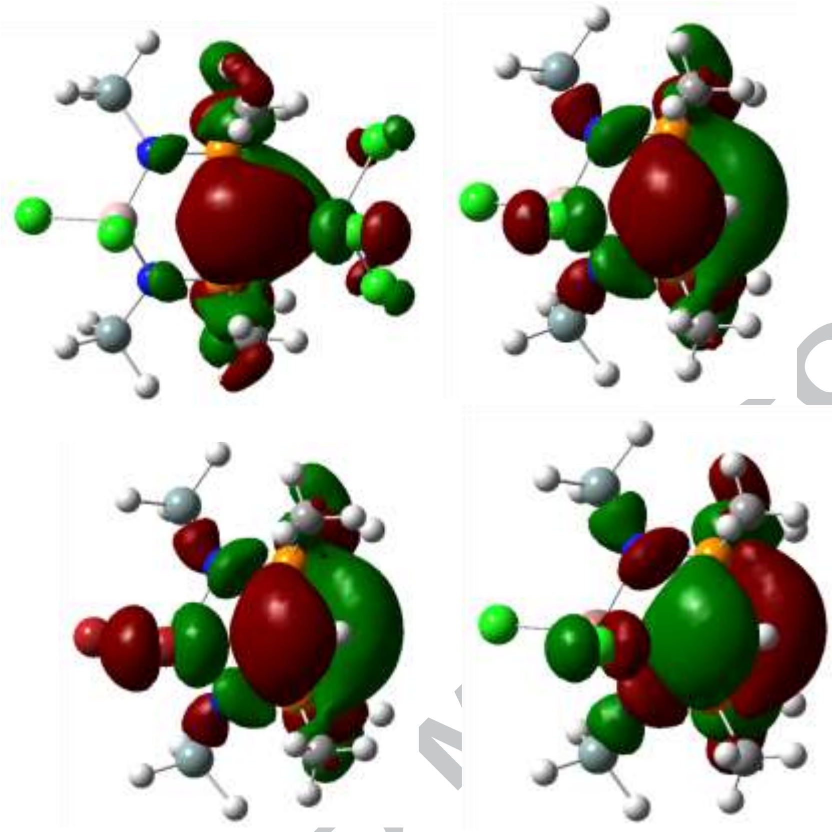

Figure 7. HOMO of $[\{C(Me_2P{=}NSiH_3)_2\}Al_2Cl_5]^-$ (**1a**) (top, left), $[\{HC(Me_2P{=}NSiH_3)_2\}AlCl_2]$ (**2a**) (top, right), $[\{HC(Me_2P{=}NSiH_3)_2\}GaBr_2]$ (**3a**) (bottom, left) and $[\{HC(Me_2P{=}NSiH_3)_2\}InCl_2]$ **(4a**) (bottom, right).

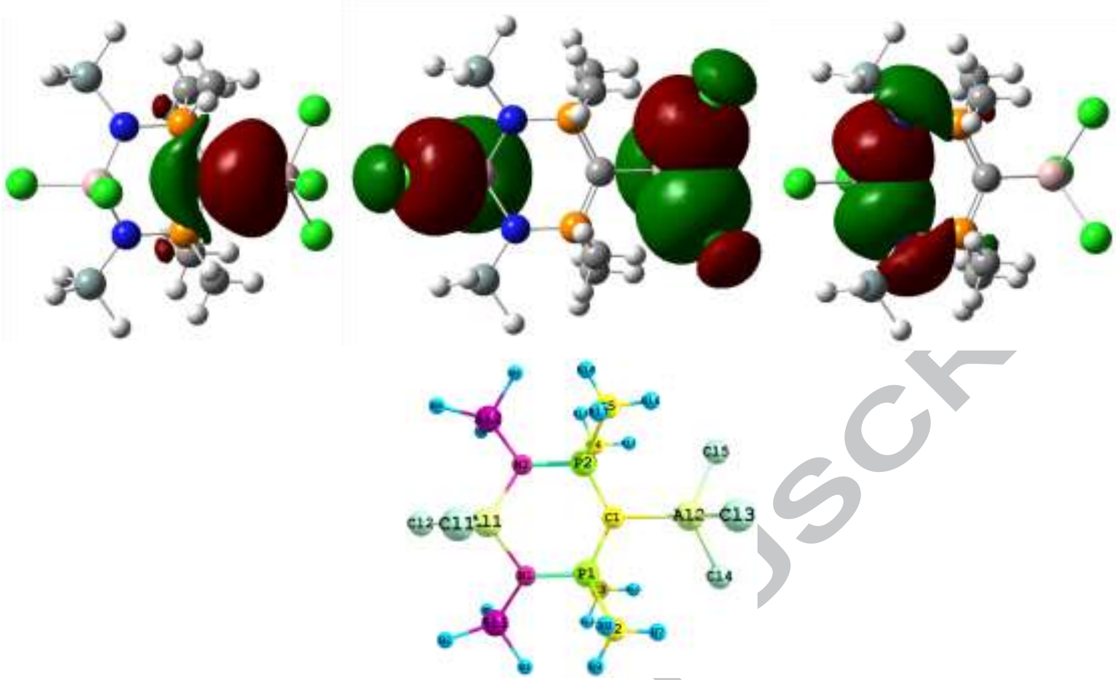

Figure 8. NBO of Al-C (top, left), Al-Cl (top, middle) and Al-N (top, right) bonds of $[\{C(Me_2P{=}NSiH_3)_2\}Al_2Cl_5]^-$ (**1a**).

Table 1. Crystal data and structure refinement details for complexes **1-6**

Empirical formula	$C_{47}H_{70}Al_2Cl_5LiN_2O_4P_2Si_2$ $2C_7H_8$ (**1**)	$C_{31}H_{39}AlCl_2N_2P_2Si_2 \cdot 2C_4H_8O$ (**2**)	$C_{31}H_{39}Br_2GaN_2P_2Si_2$ (**3**)
Formula weight	1267.59	799.85	787.30
Crystal system	Triclinic	Triclinic	Monoclinic
Crystal Dimensions	0.48×0.41×0.27 mm	0.32×0.30×0.20 mm	0.26×0.24×0.17 mm
Space group	$P\bar{1}$(No. 2)	$P\bar{1}$(No. 2)	$P2_1/c$ (No. 14)
Unit cell parameters			
a (Å)	12.933(2)	11.7241(13)	12.1720(6)
b (Å)	15.697(3)	12.1905(13)	20.8331(10)
c (Å)	17.787(3)	17.3594(19)	15.0581(8)
α (°)	73.594(2)	101.6150(14)	
β (°)	80.332(2)	100.4737(14)	113.1782(6)
γ (°)	81.510(2)	113.8145(13)	
Volume (Å^3)	3395.6(9)	2125.4(4)	3510.2(3)
Z	2	2	4
Calculated density (g cm^{-3})	1.240	1.250	1.490
Temperature, K	173.2(1)	173.2(1)	173.2(1)
μ (MoKα), (mm^{-1})	0.366	0.340	3.243
θ range for data collection (°)	0.3 to 27.54	0.3 to 26.45	0.3 to 26.36
Index ranges	$-16 \le h \le 16$ $-20 \le k \le 20$ $-23 \le l \le 23$	$-14 \le h \le 14$ $-15 \le k \le 15$ $-21 \le l \le 21$	$-15 \le h \le 15$ $-26 \le k \le 26$ $-18 \le l \le 18$
Independent reflections	15360	8688	7159
Observed reflections	9438	6448	5380
Data/restraints/parameters	15360/80/624	8688/10/467	7159/0/361
Goodness-of-fit on F^2	1.026	1.057	1.047
Final R indices			
$[F_0^2 \ge 2\sigma(F_0)]$	$R_1 = 0.0772$	$R_1 = 0.0455$	$R_1 = 0.0412$
wR_2 $[F_0^2 \ge -3\sigma(F_0^2)]$	$wR_2 = 0.2647$	$wR_2 = 0.1298$	$wR_2 = 0.1177$
Large difference peak and hole	-0.905 and 1.085 e/Å^3	-0.280 and 0.548 e/Å^3	-1.324 and 0.556 e/Å^3

Empirical formula	$C_{31}H_{39}Cl_2InN_2P_2Si_2 \cdot 2C_4H_8O$ (**4**)	$C_{31}H_{39}Br_2InN_2P_2Si_2$ (**5**)	$C_{31}H_{40}Cl_2N_2P_2Si_2$ C_4H_8O (**6**)
Formula weight	887.69	832.40	787.30
Crystal system	Triclinic	Monoclinic	Monoclinic
Crystal Dimensions	0.45×0.43×0.20 mm	0.38×0.16×0.15 mm	0.43×0.36×0.14 mm
Space group	$P\bar{1}$(No. 2)	$P2_1/c$ (No. 14)	$P2_1/m$ (No. 11)
Unit cell parameters			
a (Å)	11.9930(4)	12.3143(9)	9.1879(5)
b (Å)	12.1868(5)	20.8213(15)	20.1148(10)
c (Å)	17.7776(7)	15.2506(11)	10.7099(6)
α (°)	103.1082(4)		
β (°)	102.6668(4)	113.2510(10)	102.7190(10)
γ (°)	113.5754(4)		
Volume (Å^3)	2175.04(14)	3592.7(5)	1930.76(18)
Z	2	4	2
Calculated density (g cm^{-3})	1.355	1.539	1.32
Temperature, K	173.2(1)	173.2(1)	193.2(1)
μ (MoKα), (mm^{-1})	0.829	3.061	0.949
θ range for data collection (°)	0.3 to 27.48	0.3 to 27.51	0.3 to 27.00
Index ranges	$-15 \le h \le 15$ $-15 \le k \le 15$ $-23 \le l \le 23$	$-15 \le h \le 15$ $-27 \le k \le 26$ $-18 \le l \le 19$	$-11 \le h \le 11$ $-26 \le k \le 26$ $-13 \le l \le 13$
Independent reflections	9854	8224	4541
Observed reflections	9047	6687	4118
Data/restraints/parameters	9854/0/451	8224/0/361	4541/0/187
Goodness-of-fit on F^2	1.048	1.025	1.076
Final *R* indices			
$[F_0^2 \geq 2\sigma(F_0)]$	$R_1 = 0.0263$	$R_1 = 0.0266$	$R_1 = 0.0259$
wR_2 $[F_0^2 \geq -3\sigma(F_0^2)]$	$wR_2 = 0.0695$	$wR_2 = 0.0627$	$wR_2 = 0.0757$
Large difference peak and hole	-0.555 and 0.647 e/Å^3	-2.82 and 0.507 e/Å^3	-0.248 and 0.492 e/Å^3

Table 2. Selected bond lengths (Å) and angles (°) for compounds **1-6**

Compound **1**

Al(1)-Cl(1)	2.1460(19)	N(1)-Al(1)-N(2)	109.40(14)
Al(1)-Cl(2)	2.1684(15)	P(1)-C(1)-P(2)	116.0(2)
Al(1)-N(1)	1.866(3)	C(1)-Al(2)-Cl(3)	114.14(12)
Al(1)-N(2)	1.871(3)	C(1)-Al(2)-Cl(5)	115.38(12)
Al(2)-C(1)	1.966(4)	C(1)-P(1)-N(1)	111.94(16)
Al(2)-Cl(3)	2.1566(18)	C(1)-P(2)-N(2)	112.38(16)
Al(2)-Cl(4)	2.1665(16)	N(1)-Al(1)-Cl(1)	113.89(12)
Al(2)-Cl(5)	2.1736(15)	N(2)-Al(1)-Cl(1)	114.49(12)
C(1)-P(1)	1.728(3)	Cl(1)-Al(1)-Cl(2)	102.36(7)
C(1)-P(2)	1.727(4)	Cl(3)-Al(2)-C(4)	106.17(7)
P(1)-N(1)	1.647(3)	Cl(4)-Al(2)-Cl(5)	99.60(6)
P(2)-N(2)	1.639(3)		
C(1)-Al(1)[a]	2.957(3)		

Compound **2**

Al-Cl(1)	2.1707(9)	N(1)-Al-N(2)	113.88(9)
Al-Cl(2)	2.1688(9)	Cl(1)-Al-Cl(2)	101.65(4)
Al-N(1)	1.8818(19)	P(1)-C(1)-P(2)	123.99(14)
Al-N(2)	1.885(2)	P(1)-N(1)-Al	107.81(10)
N(1)-P(1)	1.6359(19)	P(2)-N(2)-Al	108.24(10)
N(2)-P(2)	1.6364(19)	N(1)-P(1)-C(1)	108.59(10)
C(1)-P(1)	1.713(2)	N(2)-P(2)-C(1)	108.00(11)
C(1)-P(2)	1.708(2)		
C(1)-Al[a]	2.763(3)		

Compound **3**

Ga-Br(1)	2.3529(6)	N(1)-Ga-N(2)	113.88(14)
Ga-Br(2)	2.3371(6)	Br(1)-Ga-Br(2)	105.29(2)
Ga-N(1)	1.937(3)	P(1)-C(1)-P(2)	123.0(2)
Ga-N(2)	1.922(3)	P(1)-N(1)-Ga	109.36(17)
N(1)-P(1)	1.641(3)	P(2)-N(2)-Ga	109.84(18)

N(2)-P(2)	1.642(3)	N(1)-P(1)-C(1)	111.30(18)
C(1)-P(1)	1.709(4)	N(2)-P(2)-C(1)	110.89(18)
C(1)-P(2)	1.714(4)		
C(1)-Ga[a]	2.913(3)		

Compound **4**

In-Cl(1)	2.3813(5)	N(1)-In-N(2)	108.04(6)
In-Cl(2)	2.3836(5)	Cl(1)-In-Cl(2)	100.669(19)
In-N(1)	2.1370(15)	P(1)-C(1)-P(2)	126.62(10)
In-N(2)	2.1378(14)	P(1)-N(1)-In	104.84(7)
N(1)-P(1)	1.6260(15)	P(2)-N(2)-In	104.53(7)
N(2)-P(2)	1.6260(15)	N(1)-P(1)-C(1)	108.47(8)
C(1)-P(1)	1.7283(17)	N(2)-P(2)-C(1)	109.06(8)
C(1)-P(2)	1.7289(17)		
C(1)-In[a]	2.763(3)		

Compound **5**

In-Br(1)	2.5103(4)	N(1)-In-N(2)	109.95(7)
In-Br(2)	2.5240(3)	Br(1)-In-Br(2)	105.397(11)
In-N(1)	2.1357(18)	P(1)-C(1)-P(2)	126.76(13)
In-N(2)	2.1440(18)	P(1)-N(1)-In	105.38(10)
N(1)-P(1)	1.6293(19)	P(2)-N(2)-In	104.97(9)
N(2)-P(2)	1.6297(18)	N(1)-P(1)-C(1)	109.43(10)
C(1)-P(1)	1.720(2)	N(2)-P(2)-C(1)	109.70(10)
C(1)-P(2)	1.730(2)		
C(1)-In[a]	2.803(3)		

Compound **6**

Zn-Cl(1)	2.2800(5)	N-Zn-N′	105.87(6)
Zn-Cl(2)	2.2558(5)	Cl(1)-Zn-Cl(2)	112.97(2)
Zn-N	2.0447(11)	P-C(1)-P′	119.55(9)
Zn-N′	2.0447(11)	P-N-Zn	116.84(6)
N-P	1.5887(11)	P′-N′-Zn	116.84(6)
N′-P′	1.5887(11)	N-P-C(1)	110.68(7)

C(1)-P	1.8182(9)	N′-P′-C(1)	110.68(7)
C(1)-P′	1.8183(9)		
C(1)-Zn[a]	3.156(3)		

[a] It is not directly bonding distance and indication somewhat ionic linkage separated positive/negative charge attraction interactions.

TOC Graphical Abstract

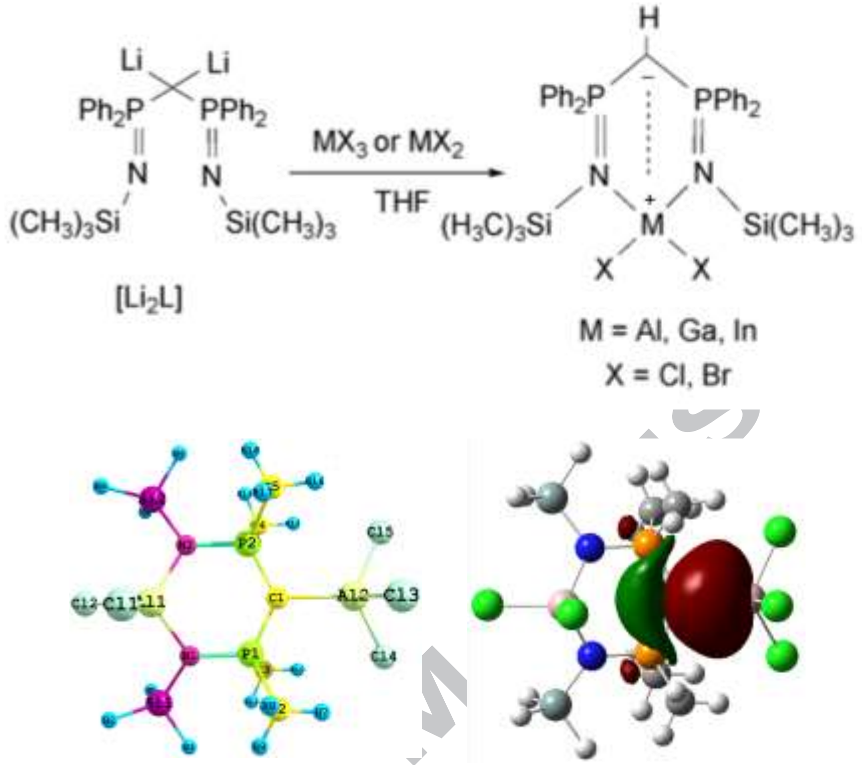

Six compounds of bis(iminophosphorano)methanide chelate ligand was synthesized and the compounds either present the intramolecular C-Al bond or C^- M^+ ionic bonding interactions.